

Characterization of Weak Collective Neural Coherence

Woochang LIM* and Sang-Yoon KIM†

Department of Physics, Kangwon National University, Chuncheon 200-701

(Received 3 September 2010, in final form 4 October 2010)

We consider a large population of N globally coupled inhibitory subthreshold neurons (which cannot fire spontaneously without noise). In a range of noise intensity, an oscillating ensemble-averaged collective potential with small amplitude emerges via cooperation of the complex potentials of individual neurons. To characterize this “weak” collective neural coherence, we introduce a new coherence measure, $M_c^{(CI)}$, based on the ensemble average of cross-correlations between the collective potential and the individual potentials. This newly-introduced measure $M_c^{(CI)}$ can be regarded as a “statistical-mechanical” measure because it quantifies the average contribution of (microscopic) individual potentials to the (macroscopic) collective potential. As a result of regular oscillations of the collective-individual cross-correlation functions, $M_c^{(CI)}$ may be used to detect weak collective coherence much better than the conventional “microscopic” measure, $M_c^{(II)}$, based on the cross-correlations between individual potentials. Furthermore, the computation load for $M_c^{(CI)}$ ($\sim N$) is much reduced as compared to that for $M_c^{(II)}$ ($\sim N^2$).

PACS numbers: 87.19.lj, 87.19.lm

Keywords: Weak collective neural coherence, Statistical-mechanical measure, Cross-correlation

DOI: 10.3938/jkps.57.1290

I. INTRODUCTION

Recently, much attention has been paid to brain rhythms [1, 2]. Synchronous neural oscillations may be used for efficient sensory processing (*e.g.*, visual binding) [3]. In addition, neural synchronization is also correlated with pathological rhythms associated with neural diseases (*e.g.*, epileptic seizures and tremors in Parkinson’s disease) [4]. Here, we are interested in the characterization of these synchronized neural rhythms.

Collective coherence in a neural population may be well described by the (population-averaged) collective potential V_C . For a coherent case, an oscillating (macroscopic) collective potential V_C emerges via cooperation of (microscopic) potentials of individual neurons. This collective neural coherence has been characterized mostly in terms of two coherence measures [5]. The first is a “thermodynamic” fluctuation-based coherence measure M_f . Neural coherence is directly related to fluctuations of the collective potential V_C . In the thermodynamic limit ($N \rightarrow \infty$), a collective state becomes coherent if an oscillating collective potential V_C appears. Otherwise (*i.e.*, when the collective potential V_C is stationary), it becomes incoherent. Thus, the mean square deviation of the collective potential V_C (*i.e.*, time-averaged fluctuations of V_C) plays the role of an order parameter to de-

scribe the coherence-incoherence transition [6]. For normalization, the order parameter is divided by the average fluctuation of individual potentials. The fluctuation-based coherence measure M_f (*i.e.*, the normalized order parameter) and the order parameter were used to characterize the degree of collective coherence in various neural systems [7–10]. Since M_f and the order parameter concern only the time-averaged fluctuations of the macroscopic potential V_C [without considering the quantitative relation between V_C and the (microscopic) individual potentials], it can be regarded as a “thermodynamic” measure. The second is a “microscopic” correlation-based measure. A cross-correlation measurement is one of the major experimental tools for studying correlations between individual potentials of pairs of neurons [11]. The cross-correlation between individual potentials of a pair of neurons is influenced not only by the direct interaction between the pair, but also by the population dynamics of the whole system [9]. For asynchronous states, the magnitude of typical cross-correlations is small (order of $1/N$) and vanishes for large N . For this asynchronous case, the cross-correlation between individual potentials of a pair of neurons depends strongly on their direct interaction. On the other hand, for synchronous states, the magnitude of typical cross-correlations is of order 1. For this synchronous case, cross-correlations are dominated by coherent population dynamics (rather than a direct interaction between a given pair). These cross-correlations may serve as a measure of collective coher-

*E-mail: wclim@kangwon.ac.kr

†Corresponding Author; E-mail: sykim@kangwon.ac.kr

ence of firing activities of neurons. Thus, a correlation-based measure $M_c^{(II)}$ given by the average of the normalized cross-correlations between individual potentials of pairs of neurons at zero-time lag was used to measure the degree of collective neural coherence [12, 13]. $M_c^{(II)}$ is a “microscopic” measure because it is based on cross-correlations between individual potentials of pairs of neurons. In addition to the characterization of collective neural coherence, a correlation-based measure was also used to characterize the spike timing reliability [14].

Many previous works for neural synchronization were done in neural systems composed of spontaneously firing (*i.e.*, self-oscillating) suprathreshold neurons. For this case, neural coherence occurs through the cooperation of regular firings of suprathreshold self-firing neurons. In contrast, neural systems composed of subthreshold neurons have received little attention. Each subthreshold neuron cannot fire spontaneously without noise (*i.e.*, it can generate firings with the aid of noise), in contrast to the suprathreshold case. Recently, collective coherence between noise-induced spikings was found in a population of pulse-coupled excitatory subthreshold neurons [15, 16]. This neural coherence emerges via cooperation of noise-induced complex firings of subthreshold neurons. The degree of neural coherence for the excitatory subthreshold case is lower than that for the suprathreshold case.

In this paper, we study collective coherence in N globally coupled inhibitory subthreshold Morris-Lecar (ML) neurons with slowly decaying synapses [17–19]. In some range of noise intensity, a coherent collective potential V_C with a small amplitude emerges via cooperation of complex individual potentials v_i ($i = 1, \dots, N$). The degree of coherence for this inhibitory subthreshold case is much lower than that for the excitatory subthreshold case. In Sec. II., we characterize this weak collective neural coherence in terms of a coherence measure $M_c^{(CI)}$ defined by the ensemble average of the cross-correlations between the collective potential V_C and the individual potentials v_i . Unlike the conventional “thermodynamic” and “microscopic” measures (M_f and $M_c^{(II)}$), this newly-introduced coherence measure $M_c^{(CI)}$ may be regarded as a “statistical-mechanical” measure because it quantifies the average contribution of (microscopic) individual potentials to the (macroscopic) collective potential. The new collective-individual cross-correlation functions exhibit distinctly regular oscillations, in contrast to the complex amplitude fluctuations of the conventional individual-individual cross-correlation functions. Such a regular oscillation implies a high-degree collective-individual correlation. Therefore, $M_c^{(CI)}$ can be used to detect weak collective coherence much better than the conventional “microscopic” measure $M_c^{(II)}$. Moreover, the computation load ($\sim N$) for $M_c^{(CI)}$ is much reduced when compared to that ($\sim N^2$) for $M_c^{(II)}$. Finally, a summary is given in Sec. III.

II. CHARACTERIZATION OF WEAK COLLECTIVE COHERENCE IN A POPULATION OF INHIBITORY SUBTHRESHOLD NEURONS

We consider an inhibitory ensemble of N globally coupled subthreshold ML neurons [17–19]. Each ML neuron with a membrane capacitance C has three intrinsic ionic currents: the calcium current I_{Ca} , the potassium current I_K , and the leakage current I_L . It is also stimulated by the common DC current I_{DC} and an independent Gaussian white noise satisfying $\langle \xi_i(t) \rangle = 0$ and $\langle \xi_i(t) \xi_j(t') \rangle = \delta_{ij} \delta(t - t')$, where $\langle \dots \rangle$ denotes the ensemble average. The noise intensity is controlled by the parameter D . Each ML neuron is connected to all the others through global synaptic couplings. Hence, it has a synaptic current I_{syn} with a synaptic reversal potential V_{syn} . The strength of the synaptic current is controlled by the parameter J , and we use $V_{syn} = -80$ mV for the inhibitory synapse.

The state of the i th neuron ($i = 1, \dots, N$) at a time t (measured in units of ms) is characterized by three state variables: the membrane potential v_i (measured in units of mV), the slow recovery variable w_i representing the activation of the K^+ current, and the synaptic gate variable s_i denoting the fraction of open synaptic ion channels. The synaptic gate variable s_i obeys the 1st-order kinetics [8, 12]. The synaptic channel opening and closing rates are $\alpha = 10$ ms $^{-1}$ and $\beta = 0.1$ ms $^{-1}$, respectively [20]. Then, the population dynamics in this neural network is governed by the following set of differential equations:

$$C \frac{dv_i}{dt} = -I_{ion,i} + I_{DC} + D\xi_i - I_{syn,i}, \quad (1a)$$

$$\frac{dw_i}{dt} = \phi \frac{(w_\infty(v_i) - w_i)}{\tau_R(v_i)}, \quad (1b)$$

$$\frac{ds_i}{dt} = \alpha s_\infty(v_i)(1 - s_i) - \beta s_i, \quad i = 1, \dots, N, \quad (1c)$$

where

$$I_{ion,i} = I_{Ca,i} + I_{K,i} + I_{L,i} \quad (2a)$$

$$= g_{Ca} m_\infty(v_i)(v_i - V_{Ca}) + g_K w_i(v_i - V_K) + g_L(v_i - V_L), \quad (2b)$$

$$I_{syn,i} = \frac{J}{N-1} \sum_{j(\neq i)}^N s_j(t)(v_i - V_{syn}), \quad (2c)$$

$$m_\infty(v) = 0.5 [1 + \tanh \{(v - V_1)/V_2\}], \quad (2d)$$

$$w_\infty(v) = 0.5 [1 + \tanh \{(v - V_3)/V_4\}], \quad (2e)$$

$$\tau_R(v) = 1 / \cosh \{(v - V_3)/(2V_4)\}, \quad (2f)$$

$$s_\infty(v_i) = 1 / (1 + e^{-v_i/2}). \quad (2g)$$

Each ionic current obeys Ohm’s law. The constants g_{Ca} , g_K , and g_L are the maximum conductances for the ion and leakage channels, and the constants V_{Ca} , V_K , and V_L are the reversal potentials. As is well known, the ML

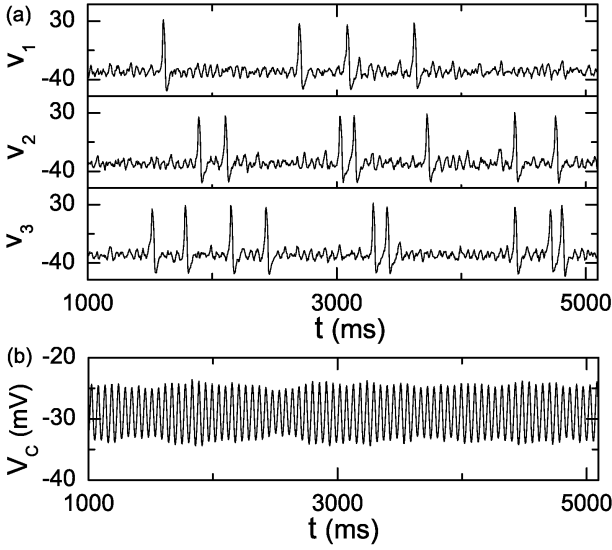


Fig. 1. Individual and collective membrane potentials in $N(=10^3)$ globally coupled inhibitory subthreshold ML neurons for $I_{DC} = 87 \mu\text{A}/\text{cm}^2$, $D = 20 \mu\text{A} \cdot \text{ms}^{1/2}/\text{cm}^2$, and $J = 3 \text{ mS}/\text{cm}^2$: (a) time series of three individual potentials v_1 , v_2 , and v_3 (unit of potential: mV), and (b) time series of the ensemble-averaged collective potential V_C with small amplitude.

neuron may exhibit either type-I or type-II excitability, depending on the system parameters. Throughout this paper, we consider the case of type-II excitability with the parameter values given in Ref. 18. Numerical integration of Eq. (1) is done using the Heun method [21] with the time step $\Delta t = 0.01 \text{ ms}$, and data for (v_i, w_i, s_i) ($i = 1, \dots, N$) are obtained with the sampling time interval $\Delta t = 1 \text{ ms}$.

We study collective coherence in an inhibitory population of $N (= 10^3)$ globally coupled subthreshold ML neurons by varying the noise intensity D for $I_{DC} = 87 \mu\text{A}/\text{cm}^2$ and $J = 3 \text{ mS}/\text{cm}^2$. (Hereafter, for convenience, we omit the dimensions of I_{DC} , D , and J .) Emergence of collective coherence in the population may be well described by the population-averaged collective potential

$$V_C(t) = \frac{1}{N} \sum_{i=1}^N v_i(t). \quad (3)$$

For $9.4 < D < 33.4$, an oscillating collective potential V_C with small amplitude appears [22]. As an example, we consider the weakly coherent case of $D = 20$. Figure 1 shows individual potentials of the first three neurons and the collective potential V_C . Individual inhibitory neurons exhibit intermittent firings phase-locked to V_C at random multiples of the period $T (=54.2 \text{ ms})$ of V_C . However, through cooperation of these complex individual potentials, a regularly oscillating collective potential V_C with small amplitude emerges.

We characterize the weak collective coherence for the case of $D = 20$ in terms of the cross-correlations between

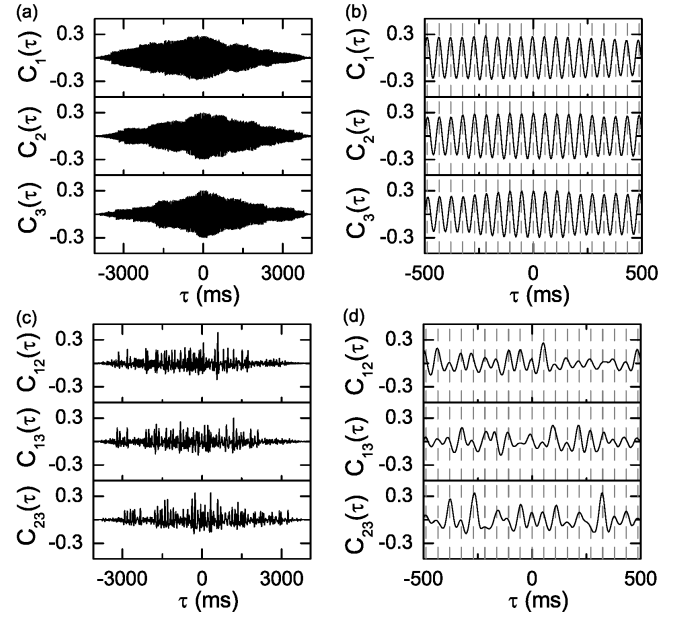


Fig. 2. Collective-individual and individual-individual cross-correlation functions in $N(=10^3)$ globally coupled inhibitory subthreshold ML neurons for $I_{DC} = 87 \mu\text{A}/\text{cm}^2$, $D = 20 \mu\text{A} \cdot \text{ms}^{1/2}/\text{cm}^2$, and $J = 3 \text{ mS}/\text{cm}^2$: (a) cross-correlation functions $C_i(\tau)$ between the collective potential V_C and the individual potential v_i ($i = 1, 2, 3$), (b) magnifications of $C_i(\tau)$ near $\tau = 0$, (c) cross-correlation functions $C_{ij}(\tau)$ between individual potentials v_i and v_j for the first three neurons, and (d) magnifications of $C_{ij}(\tau)$ near $\tau = 0$. Vertical dashed lines in (b) and (d) represent the integer multiples of the period $T (=54.2 \text{ ms})$ of V_C . The number of data used for the calculation of each cross-correlation function in (a) and (c) is 2^{12} .

the collective potential V_C and the individual potentials v_i ($i = 1, \dots, N$); thus, we make clear the quantitative relation between the (macroscopic) collective potential V_C and the (microscopic) individual potentials. The normalized cross-correlation function $C_i(\tau)$ between V_C and v_i is given by

$$C_i(\tau) = \frac{\overline{\Delta V_C(t+\tau) \Delta v_i(t)}}{\sqrt{\overline{\Delta V_C^2(t)}} \sqrt{\overline{\Delta v_i^2(t)}}}, \quad (4)$$

where τ is the time lag, $\Delta V_C(t) = V_C(t) - \overline{V_C(t)}$, $\Delta v_i(t) = v_i(t) - \overline{v_i(t)}$, and the overline denotes the time average. The first three cross-correlation functions $C_i(\tau)$ between V_C and v_i ($i = 1, 2, 3$) are shown in Fig. 2(a). They exhibit nearly regularly-damped oscillations with decaying amplitudes for large time lag τ . As shown in Fig. 2(b), the $C_i(\tau)$'s exhibit in-phase oscillations because they are phase-locked to V_C . For comparison, we also obtain the conventional cross-correlation functions $C_{ij}(\tau)$ between individual potentials v_i and v_j :

$$C_{ij}(\tau) = \frac{\overline{\Delta v_i(t+\tau) \Delta v_j(t)}}{\sqrt{\overline{\Delta v_i^2(t)}} \sqrt{\overline{\Delta v_j^2(t)}}}, \quad (5)$$

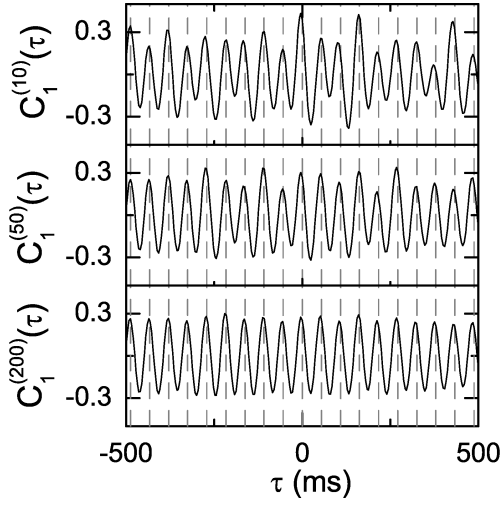


Fig. 3. Convergence of the k th-order approximant $C_1^{(k)}(\tau)$ to the cross-correlation function $C_1(\tau)$ between V_C and v_1 in $N (= 10^3)$ globally coupled inhibitory subthreshold ML neurons for $I_{DC} = 87 \mu\text{A}/\text{cm}^2$, $D = 20 \mu\text{A} \cdot \text{ms}^{1/2}/\text{cm}^2$, and $J = 3 \text{mS}/\text{cm}^2$. Vertical dashed lines denote integer multiples of the period $T (= 54.2 \text{ms})$ of V_C . The number of data used for the calculation of each k th-order approximant $C_1^{(k)}(\tau)$ is 2^{12} .

where $\Delta v_i(t) = v_i(t) - \overline{v_i(t)}$. Unlike the “regular” cross-correlation functions C_i between V_C and v_i , the cross-correlation functions C_{ij} between the individual potentials show apparently “irregular” oscillations due to amplitude fluctuations (see Fig. 2(c)). However, their phases are locked to V_C due to the effect of coherent population dynamics, as shown in Fig. 2(d). The regular oscillation of the cross-correlation function C_i implies a high-degree collective-individual correlation. Hence, weak collective coherence may be detected in the collective-individual cross-correlation function C_i much better than in the conventional individual-individual cross-correlation function C_{ij} .

We expect averaging of the individual-individual cross-correlation functions to lead to a regular oscillation as in the case of the collective-individual cross-correlation function. To show this explicitly, we rewrite the collective-individual cross-correlation function C_i of Eq. (4) as a summation of unnormalized individual-individual cross-correlations:

$$C_i(\tau) = \frac{\sum_{j=1}^N \overline{\Delta v_j(t+\tau) \Delta v_i(t)}}{N \sqrt{\overline{\Delta V_C^2(t)}} \sqrt{\overline{\Delta v_i^2(t)}}}. \quad (6)$$

Figure 3 shows three k th-order ($k = 10, 50, \text{ and } 200$) approximants, $C_i^{(k)}(\tau)$, to the collective-individual cross-correlation function $C_i(\tau)$, where

$$C_i^{(k)}(\tau) = \frac{\sum_{j=1}^k \overline{\Delta v_j(t+\tau) \Delta v_i(t)}}{k \sqrt{\overline{\Delta V_C^2(t)}} \sqrt{\overline{\Delta v_i^2(t)}}}. \quad (7)$$

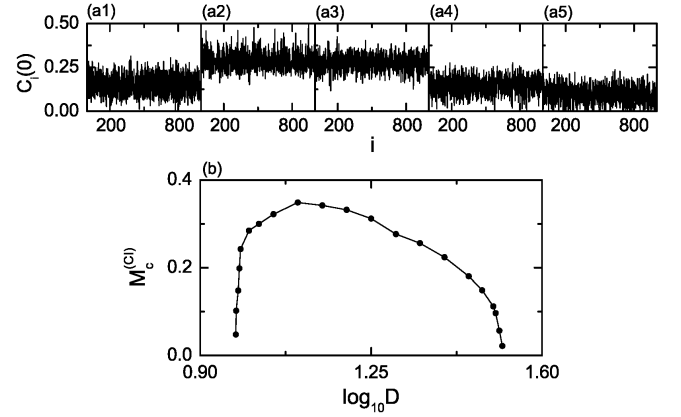


Fig. 4. “Statistical-mechanical” measure $M_c^{(CT)}$ based on the collective-individual correlations in $N (= 10^3)$ globally coupled inhibitory subthreshold ML neurons for $I_{DC} = 87 \mu\text{A}/\text{cm}^2$ and $J = 3 \text{mS}/\text{cm}^2$. (a) Plots of $C_i(0)$ (cross-correlation at the zero-time lag between V_C and v_i) versus i (neuron) for (a1) $D = 9.5 \mu\text{A} \cdot \text{ms}^{1/2}/\text{cm}^2$, (a2) $D = 10 \mu\text{A} \cdot \text{ms}^{1/2}/\text{cm}^2$, (a3) $D = 20 \mu\text{A} \cdot \text{ms}^{1/2}/\text{cm}^2$, (a4) $D = 30 \mu\text{A} \cdot \text{ms}^{1/2}/\text{cm}^2$, and (a5) $D = 32 \mu\text{A} \cdot \text{ms}^{1/2}/\text{cm}^2$. (b) Plot of $M_c^{(CT)}$ versus $\log_{10} D$. The number of data used for the calculation of a cross-correlation function for each D in (a) and (b) is 2^{12} .

As the order k is increased, more regular oscillations appear.

To quantify the weak collective neural coherence, we introduce a coherence measure $M_c^{(CT)}$ based on the collective-individual cross-correlations $C_i(0)$ between V_C and v_i at zero-time lag:

$$M_c^{(CT)} = \frac{1}{N} \sum_{i=1}^N C_i(0). \quad (8)$$

Unlike the conventional “microscopic” measure $M_c^{(IT)}$, $M_c^{(CT)}$ may be regarded as a “statistical-mechanical” measure because it quantifies the average contribution of (microscopic) individual potentials to the (macroscopic) collective potential. By varying D in the coherent region ($9.4 < D < 33.4$), we measure the degree of weak collective coherence in terms of $M_c^{(CT)}$. Figure 4(a) shows plots of $C_i(0)$ versus i (neuron index) for various values of D ; for each value of D , fluctuations occur at about the average value. By averaging $C_i(0)$ over all neurons for each value of D , we obtain a bell-shaped graph of $M_c^{(CT)}$ (see Fig. 4(b)). A maximal collective coherence is found to occur for $D = D^* (\simeq 13)$. We also discuss the effect of collective coherence on individual subthreshold neurons. Due to the stochastic spiking coherence, the synaptic current, injected into each individual neuron, becomes temporally coherent. Hence, the stochastic resonance of an individual subthreshold neuron in the network may be enhanced [23]. The degree of the stochastic resonance is also maximal for $D = D^*$. As a result of

the regular oscillations of the collective-individual cross-correlation functions C_i (see Fig. 2), the “statistical-mechanical” measure $M_c^{(CI)}$ may be used to detect weak collective coherence much better than the conventional “microscopic” measure $M_c^{(II)}$. Furthermore, the computation load for $M_c^{(CI)}$ increases in proportion to N because of the ensemble average over all neurons while that for $M_c^{(II)}$ grows in proportion to N^2 due to the average over all neuron pairs. Hence, the computation load ($\sim N$) for $M_c^{(CI)}$ is much reduced as compared to that ($\sim N^2$) for $M_c^{(II)}$.

III. SUMMARY

We have studied weak collective coherence in a population of N globally coupled inhibitory subthreshold ML neurons. For a weakly coherent case, a regularly oscillating collective potential V_C with small amplitude appears through cooperation of complex individual potentials. To characterize this weak collective neural coherence, we introduce a new type of “statistical-mechanical” coherence measure, $M_c^{(CI)}$, by considering the average cross-correlations between the collective potential V_C and the individual potentials v_i ($i = 1, \dots, N$). We note that the new collective-individual cross-correlation functions exhibit distinctly regular oscillations while the conventional individual-individual cross-correlation functions show complex amplitude fluctuations. This regular oscillation implies a high-degree of collective-individual correlation. Hence, $M_c^{(CI)}$ can be used to detect the weak collective coherence much better than the conventional “microscopic” measure $M_c^{(II)}$ based on the individual-individual correlations. Moreover, the computation load ($\sim N$) for $M_c^{(CI)}$ is much reduced when compared to that ($\sim N^2$) for $M_c^{(II)}$. Finally, we expect that $M_c^{(CI)}$ to possibly be implemented to characterize the weak collective neural coherence in the experimentally-obtained data of individual and collective potentials.

ACKNOWLEDGMENTS

This research was supported by the Basic Science Research Program through the National Research Foundation of Korea funded by the Ministry of Education, Science and Technology (2009-0070865).

REFERENCES

- [1] G. Buzsáki, *Rhythms of the Brain* (Oxford University Press, New York, 2006).
- [2] X.-J. Wang, *Encyclopedia of Cognitive Science*, edited by L. Nadel (MacMillan, London, 2003), p. 272.
- [3] C. M. Gray, *J. Comput. Neurosci.* **1**, 11 (1994).
- [4] B. Hauschildt, N. B. Janson, A. Balanov and E. Schöll, *Phys. Rev. E* **74**, 051906 (2006); P. Grosse, M. J. Cassidy and P. Brown, *Clin. Neurophysiol.* **113**, 1523 (2002); P. Tass, M. G. Rosenblum, J. Weule, J. Kurths, A. Pikovsky, J. Volkman, A. Schnitzler and H. J. Freund, *Phys. Rev. Lett.* **81**, 3291 (1998).
- [5] D. Golomb, *Scholarpedia* **2**, 1347 (2007).
- [6] S. C. Manrubia, A. S. Mikhailov and D. H. Zanette, *Emergence of Dynamical Order* (World Scientific, Singapore, 2004).
- [7] D. Hansel and H. Sompolinsky, *Phys. Rev. Lett.* **68**, 718 (1992).
- [8] D. Golomb and J. Rinzel, *Phys. Rev. E* **48**, 4810 (1993); *Physica D* **72**, 259 (1994).
- [9] I. Ginzburg and H. Sompolinsky, *Phys. Rev. E* **50**, 3171 (1994).
- [10] D. Hansel and G. Mato, *Neural Comput.* **15**, 1 (2003).
- [11] M. Abeles, *Corticonics: Neural Circuits of the Cerebral Cortex* (Cambridge University Press, Cambridge, 1991).
- [12] X.-J. Wang and G. Buzsáki, *J. Neurosci.* **16**, 6402 (1996).
- [13] J. White, C. C. Chow, J. Ritt, C. Soto-Trevino and N. Kopell, *J. Comput. Neurosci.* **5**, 5 (1998).
- [14] S. Schreiber, J. M. Fellous, D. Whitmer, P. Tiesinga and T. J. Sejnowski, *Neurocomputing* **52**, 925 (2003).
- [15] Y. Wang, D. T. W. Chik and Z. D. Wang, *Phys. Rev. E* **61**, 740 (2000).
- [16] W. Lim and S.-Y. Kim, *J. Korean Phys. Soc.* **51**, 1427 (2007); *Int. J. Mod. Phys. B* **23**, 703 (2009).
- [17] C. Morris and H. Lecar, *Biophys. J.* **35**, 193 (1981).
- [18] J. Rinzel and B. Ermentrout, *Methods in Neural Modeling: from Ions to Networks*, edited by C. Koch and I. Segev (MIT Press, Cambridge, 1998), p. 251.
- [19] K. Tsumoto, H. Kitajima, T. Yoshinaga, K. Aihara and H. Kawakami, *Neurocomput.* **69**, 293 (2006).
- [20] C. Börgers and N. Kopell, *Neural Comput.* **15**, 509 (2003); *ibid.* **17**, 557 (2005).
- [21] M. San Miguel and R. Toral, in *Instabilities and Nonequilibrium Structures VI*, edited by J. Martinez, R. Tieemann and E. Tirapegui (Kluwer Academic Publisher, Dordrecht, 2000), p. 35.
- [22] W. Lim and S.-Y. Kim (unpublished). For $9.4 < D < 33.4$, coherent states exist because the order parameter (*i.e.*, the mean square deviation of the collective potential) approaches a non-zero limit as the number of neurons goes to infinity.
- [23] L. Gammaitoni, P. Hänggi, P. Jung and F. Marchesoni, *Rev. Mod. Phys.* **70**, 223 (1998).